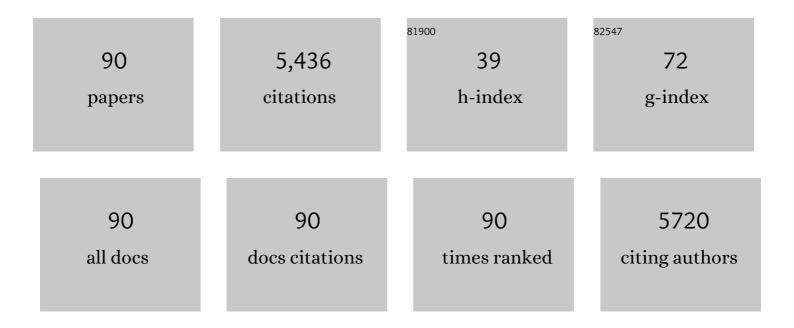
Yongbing Xie

List of Publications by Year in descending order

Source: https://exaly.com/author-pdf/5073296/publications.pdf Version: 2024-02-01



YONCRING XIE

#	Article	IF	CITATIONS
1	A facial synthesis of nitrogen-doped reduced graphene oxide quantum dot and its application in aqueous organics degradation. Green Energy and Environment, 2022, 7, 440-448.	8.7	9
2	Ni nanoparticles encapsulated within H-type ZSM-5 crystals for upgrading palmitic acid to diesel-like fuels. Chinese Chemical Letters, 2022, 33, 803-806.	9.0	9
3	In-situ synthesis of N, S co-doped hollow carbon microspheres for efficient catalytic oxidation of organic contaminants. Chinese Chemical Letters, 2022, 33, 1298-1302.	9.0	20
4	Facile synthesis of nitrogen and sulfur co-doped hollow microsphere polymers from benzothiazole containing wastewater for water treatment. Chemosphere, 2022, 287, 131982.	8.2	2
5	Mechanism of ozone adsorption and activation on B-, N-, P-, and Si-doped graphene: A DFT study. Chemical Engineering Journal, 2022, 430, 133114.	12.7	27
6	A promising catalytic solution of NO reduction by CO using g-C3N4/TiO2: A DFT study. Journal of Colloid and Interface Science, 2022, 610, 152-163.	9.4	7
7	Degradation of potassium alkyl xanthogenate in wet air oxidation: Enhancement method, degradation mechanism and structure impact. Journal of Environmental Chemical Engineering, 2022, 10, 107349.	6.7	4
8	Activated carbon adsorption coupled with ozonation regeneration for efficient removal of chlorobenzene. Journal of Environmental Chemical Engineering, 2022, 10, 107319.	6.7	19
9	The structure-activity relationship of aromatic compounds in advanced oxidation processes:a review. Chemosphere, 2022, 296, 134071.	8.2	18
10	Insights into the Mechanism of Ozone Activation and Singlet Oxygen Generation on N-Doped Defective Nanocarbons: A DFT and Machine Learning Study. Environmental Science & Technology, 2022, 56, 7853-7863.	10.0	27
11	Boosting oxygen evolution reactivity by modulating electronic structure and honeycomb-like architecture in Ni2P/N,P-codoped carbon hybrids. Green Energy and Environment, 2021, 6, 866-874.	8.7	12
12	Conversion of phenol to cyclohexane in the aqueous phase over Ni/zeolite bi-functional catalysts. Frontiers of Chemical Science and Engineering, 2021, 15, 288-298.	4.4	16
13	Mechanistic Investigations of the Pyridinic N–Co Structures in Co Embedded N-Doped Carbon Nanotubes for Catalytic Ozonation. ACS ES&T Engineering, 2021, 1, 32-45.	7.6	50
14	Upgrading of palmitic acid to diesel-like fuels over Ni@HZSM-5 bi-functional catalysts through the in situ encapsulation method. Molecular Catalysis, 2021, 511, 111715.	2.0	9
15	Encapsulated Ni Nanoparticles within Silicalite-1 Crystals for Upgrading Phenolic Compounds to Arenes. Industrial & Engineering Chemistry Research, 2021, 60, 13790-13801.	3.7	3
16	Different roles of Fe atoms and nanoparticles on g-C3N4 in regulating the reductive activation of ozone under visible light. Applied Catalysis B: Environmental, 2021, 296, 120362.	20.2	54
17	N-dependent ozonation efficiency over nitrogen-containing heterocyclic contaminants: A combined density functional theory study on reaction kinetics and degradation pathways. Chemical Engineering Journal, 2020, 382, 122708.	12.7	33
18	The duet of surface and radical-based carbocatalysis for oxidative destructions of aqueous contaminants over built-in nanotubes of graphite. Journal of Hazardous Materials, 2020, 384, 121486.	12.4	29

#	Article	IF	CITATIONS
19	Support effect boosting the electrocatalytic N ₂ reduction activity of Ni ₂ P/N,P-codoped carbon nanosheet hybrids. Journal of Materials Chemistry A, 2020, 8, 2691-2700.	10.3	32
20	Degradation of phenolic compounds by dielectric barrier plasma: Process optimization and influence of phenol substituents. Chemical Engineering Journal, 2020, 385, 123732.	12.7	42
21	Iron/nickel nano-alloy encapsulated in nitrogen-doped carbon framework for CO2 electrochemical conversion with prominent CO selectivity. Journal of Power Sources, 2020, 449, 227496.	7.8	10
22	Coupling-oxidation process promoted ring-opening degradation of 2-mecapto-5-methyl-1,3,4-thiadizaole in wastewater. Water Research, 2020, 186, 116362.	11.3	7
23	Nanocarbon-Based Catalytic Ozonation for Aqueous Oxidation: Engineering Defects for Active Sites and Tunable Reaction Pathways. ACS Catalysis, 2020, 10, 13383-13414.	11.2	141
24	Br/Co/N Co-doped porous carbon frameworks with enriched defects for high-performance electrocatalysis. Journal of Materials Chemistry A, 2020, 8, 10865-10874.	10.3	47
25	Efficient Tetra-Functional Electrocatalyst with Synergetic Effect of Different Active Sites for Multi-Model Energy Conversion and Storage. ACS Applied Materials & Interfaces, 2020, 12, 23017-23027.	8.0	12
26	Visible-Light Photocatalytic Ozonation Using Graphitic C ₃ N ₄ Catalysts: A Hydroxyl Radical Manufacturer for Wastewater Treatment. Accounts of Chemical Research, 2020, 53, 1024-1033.	15.6	81
27	Reactive Oxygen Species and Catalytic Active Sites in Heterogeneous Catalytic Ozonation for Water Purification. Environmental Science & Technology, 2020, 54, 5931-5946.	10.0	285
28	Metal-free catalytic ozonation on surface-engineered graphene: Microwave reduction and heteroatom doping. Chemical Engineering Journal, 2019, 355, 118-129.	12.7	86
29	Dendritic BiVO4 decorated with MnOx co-catalyst as an efficient hierarchical catalyst for photocatalytic ozonation. Frontiers of Chemical Science and Engineering, 2019, 13, 185-191.	4.4	17
30	Number of Reactive Charge Carriers—A Hidden Linker between Band Structure and Catalytic Performance in Photocatalysts. ACS Catalysis, 2019, 9, 8852-8861.	11.2	31
31	Single-Atom Mn–N ₄ Site-Catalyzed Peroxone Reaction for the Efficient Production of Hydroxyl Radicals in an Acidic Solution. Journal of the American Chemical Society, 2019, 141, 12005-12010.	13.7	203
32	Selective Production of Jet-Fuel-Range Alkanes from Palmitic Acid over Ni/H-MCM-49 with Two Independent Pore Systems. Industrial & Engineering Chemistry Research, 2019, 58, 21341-21349.	3.7	14
33	Role of oxygen vacancies and Mn sites in hierarchical Mn2O3/LaMnO3-δ perovskite composites for aqueous organic pollutants decontamination. Applied Catalysis B: Environmental, 2019, 245, 546-554.	20.2	187
34	Hierarchical biomimetic BiVO4 for the treatment of pharmaceutical wastewater in visible-light photocatalytic ozonation. Chemosphere, 2019, 222, 38-45.	8.2	55
35	Occurrence of both hydroxyl radical and surface oxidation pathways in N-doped layered nanocarbons for aqueous catalytic ozonation. Applied Catalysis B: Environmental, 2019, 254, 283-291.	20.2	109
36	Temperature-Dependent Selectivity of Hydrogenation/Hydrogenolysis during Phenol Conversion over Ni Catalysts. ACS Sustainable Chemistry and Engineering, 2019, 7, 9464-9473.	6.7	31

#	Article	IF	CITATIONS
37	Enhanced removal of benzothiazole in persulfate promoted wet air oxidation via degradation and synchronous polymerization. Chemical Engineering Journal, 2019, 370, 208-217.	12.7	14
38	Acidity induced fast transformation of acetaminophen by different MnO2: Kinetics and pathways. Chemical Engineering Journal, 2019, 359, 518-529.	12.7	21
39	Distinct synergetic effects in the ozone enhanced photocatalytic degradation of phenol and oxalic acid with Fe 3+ /TiO 2 catalyst. Chinese Journal of Chemical Engineering, 2018, 26, 1528-1535.	3.5	12
40	Reaction condition optimization and degradation pathway in wet oxidation of benzopyrazole revealed by computational and experimental approaches. Journal of Hazardous Materials, 2018, 351, 169-176.	12.4	6
41	Tailored synthesis of active reduced graphene oxides from waste graphite: Structural defects and pollutant-dependent reactive radicals in aqueous organics decontamination. Applied Catalysis B: Environmental, 2018, 229, 71-80.	20.2	128
42	Wet air oxidation of indole, benzopyrazole, and benzotriazole: Effects of operating conditions and reaction mechanisms. Chemical Engineering Journal, 2018, 338, 496-503.	12.7	18
43	Promising application of SiC without co-catalyst in photocatalysis and ozone integrated process for aqueous organics degradation. Catalysis Today, 2018, 315, 223-229.	4.4	17
44	High activity of g-C3N4/multiwall carbon nanotube in catalytic ozonation promotes electro-peroxone process. Chemosphere, 2018, 201, 206-213.	8.2	42
45	Enhanced hole-dominated photocatalytic activity of doughnut-like porous g-C3N4 driven by down-shifted valance band maximum. Catalysis Today, 2018, 307, 147-153.	4.4	25
46	Phenolic compounds removal by wet air oxidation based processes. Frontiers of Environmental Science and Engineering, 2018, 12, 1.	6.0	46
47	Towards a better understanding of the synergistic effect in the electro-peroxone process using a three electrode system. Chemical Engineering Journal, 2018, 337, 733-740.	12.7	26
48	C ₃ N ₄ –Mn/CNT composite as a heterogeneous catalyst in the electro-peroxone process for promoting the reaction between O ₃ and H ₂ O ₂ in acid solution. Catalysis Science and Technology, 2018, 8, 6241-6251.	4.1	10
49	The role of ozone and influence of band structure in WO3 photocatalysis and ozone integrated process for pharmaceutical wastewater treatment. Journal of Hazardous Materials, 2018, 360, 481-489.	12.4	60
50	Chloro-benquinone Modified on Graphene Oxide as Metal-free Catalyst: Strong Promotion of Hydroxyl Radical and Generation of Ultra-Small Graphene Oxide. Scientific Reports, 2017, 7, 42643.	3.3	16
51	Selection of active phase of MnO2 for catalytic ozonation of 4-nitrophenol. Chemosphere, 2017, 168, 1457-1466.	8.2	159
52	ls C ₃ N ₄ Chemically Stable toward Reactive Oxygen Species in Sunlight-Driven Water Treatment?. Environmental Science & Technology, 2017, 51, 13380-13387.	10.0	119
53	Fast Electron Transfer and [•] OH Formation: Key Features for High Activity in Visible-Light-Driven Ozonation with C ₃ N ₄ Catalysts. ACS Catalysis, 2017, 7, 6198-6206.	11.2	135
54	Synthesis of Magnetic Carbon Supported Manganese Catalysts for Phenol Oxidation by Activation of Peroxymonosulfate. Catalysts, 2017, 7, 3.	3.5	10

#	Article	IF	CITATIONS
55	Towards effective design of active nanocarbon materials for integrating visible-light photocatalysis with ozonation. Carbon, 2016, 107, 658-666.	10.3	52
56	Novel oxidative cutting graphene oxide to graphene quantum dots for electrochemical sensing application. Materials Today Communications, 2016, 8, 127-133.	1.9	33
57	The influence of the substituent on the phenol oxidation rate and reactive species in cubic MnO ₂ catalytic ozonation. Catalysis Science and Technology, 2016, 6, 7875-7884.	4.1	57
58	Superoxide radical-mediated photocatalytic oxidation of phenolic compounds over Ag + /TiO 2 : Influence of electron donating and withdrawing substituents. Journal of Hazardous Materials, 2016, 304, 126-133.	12.4	82
59	Enhanced proton and electron reservoir abilities of polyoxometalate grafted on graphene for high-performance hydrogen evolution. Energy and Environmental Science, 2016, 9, 1012-1023.	30.8	138
60	Insights into the mechanism of phenolic mixture degradation by catalytic ozonation with a mesoporous Fe ₃ O ₄ /MnO ₂ composite. RSC Advances, 2016, 6, 29674-29684.	3.6	32
61	Efficient Catalytic Ozonation over Reduced Graphene Oxide for <i>p</i> -Hydroxylbenzoic Acid (PHBA) Destruction: Active Site and Mechanism. ACS Applied Materials & Interfaces, 2016, 8, 9710-9720.	8.0	234
62	Hierarchical shape-controlled mixed-valence calcium manganites for catalytic ozonation of aqueous phenolic compounds. Catalysis Science and Technology, 2016, 6, 2918-2929.	4.1	69
63	Dramatic coupling of visible light with ozone on honeycomb-like porous g-C 3 N 4 towards superior oxidation of water pollutants. Applied Catalysis B: Environmental, 2016, 183, 417-425.	20.2	165
64	Disparate roles of doped metal ions in promoting surface oxidation of TiO 2 photocatalysis. Journal of Photochemistry and Photobiology A: Chemistry, 2016, 315, 59-66.	3.9	38
65	Super synergy between photocatalysis and ozonation using bulk g-C3N4 as catalyst: A potential sunlight/O3/g-C3N4 method for efficient water decontamination. Applied Catalysis B: Environmental, 2016, 181, 420-428.	20.2	113
66	2D/2D nano-hybrids of γ-MnO 2 on reduced graphene oxide for catalytic ozonation and coupling peroxymonosulfate activation. Journal of Hazardous Materials, 2016, 301, 56-64.	12.4	195
67	g-C3N4-triggered super synergy between photocatalysis and ozonation attributed to promoted OH generation. Catalysis Communications, 2015, 66, 10-14.	3.3	57
68	Catalytic ozonation of 4-nitrophenol over an mesoporous α-MnO2 with resistance to leaching. Catalysis Today, 2015, 258, 595-601.	4.4	88
69	A closed-loop process for recycling LiNi1/3Co1/3Mn1/3O2 from the cathode scraps of lithium-ion batteries: Process optimization and kinetics analysis. Separation and Purification Technology, 2015, 150, 186-195.	7.9	169
70	Organic pollutants removal in wastewater by heterogeneous photocatalytic ozonation. Chemosphere, 2015, 121, 1-17.	8.2	282
71	Mechanisms of Cu ²⁺ migration, recovery and detoxification in Cu ²⁺ -, -containing wastewater treatment process with anaerobic granular sludge. Environmental Technology (United Kingdom), 2014, 35, 1956-1961.	2.2	11
72	The evolution of surface charge on graphene oxide during the reduction and its application in electroanalysis. Carbon, 2014, 66, 302-311.	10.3	134

#	Article	IF	CITATIONS
73	Activated carbon-enhanced ozonation of oxalate attributed to HO oxidation in bulk solution and surface oxidation: Effects of the type and number of basic sites. Chemical Engineering Journal, 2014, 245, 71-79.	12.7	45
74	Capacitive deionization by ordered mesoporous carbon: electrosorption isotherm, kinetics, and the effect of modification. Desalination and Water Treatment, 2014, 52, 1388-1395.	1.0	15
75	Promoting effect of nitration modification on activated carbon in the catalytic ozonation of oxalic acid. Applied Catalysis B: Environmental, 2014, 146, 169-176.	20.2	99
76	Reaction mechanism and metal ion transformation in photocatalytic ozonation of phenol and oxalic acid with Ag+/TiO2. Journal of Environmental Sciences, 2014, 26, 662-672.	6.1	23
77	Graphene–CdS quantum dots–polyoxometalate composite films for efficient photoelectrochemical water splitting and pollutant degradation. Physical Chemistry Chemical Physics, 2014, 16, 26016-26023.	2.8	27
78	A novel process for recycling and resynthesizing LiNi1/3Co1/3Mn1/3O2 from the cathode scraps intended for lithium-ion batteries. Waste Management, 2014, 34, 1715-1724.	7.4	111
79	Activated carbon enhanced ozonation of oxalate attributed to HO oxidation in bulk solution and surface oxidation: Effect of activated carbon dosage and pH. Journal of Environmental Sciences, 2014, 26, 2095-2105.	6.1	15
80	An overview on the processes and technologies for recycling cathodic active materials from spent lithium-ion batteries. Journal of Material Cycles and Waste Management, 2013, 15, 420-430.	3.0	163
81	Double layered, one-pot hydrothermal synthesis of M-TiO2 (M = Fe3+, Ni2+, Cu2+ and Co2+) and their application in photocatalysis. Science China Chemistry, 2013, 56, 1783-1789.	8.2	14
82	Coagulation behaviors and in-situ flocs characteristics of composite coagulants in cyanide-containing wastewater: Role of cationic polyelectrolyte. Science China Chemistry, 2013, 56, 1765-1774.	8.2	3
83	Morphologic evolution of Au nanocrystals grown in ionic liquid by plasma reduction. Journal of Colloid and Interface Science, 2012, 374, 40-44.	9.4	21
84	Highly Selective PdCu/Amorphous Silicaâ^'Alumina (ASA) Catalysts for Groundwater Denitration. Environmental Science & Technology, 2011, 45, 4066-4072.	10.0	48
85	Enhanced Activity of Bimetallic Pd-Based Catalysts for Methane Combustion. Catalysis Letters, 2008, 125, 130-133.	2.6	16
86	Stability of Ionic Liquids under the Influence of Glow Discharge Plasmas. Plasma Processes and Polymers, 2008, 5, 239-245.	3.0	44
87	Stability of Pt particles on ZrO2 support during partial oxidation of methane: DRIFT studies of adsorbed CO. Journal of Molecular Catalysis A, 2008, 282, 67-73.	4.8	13
88	Carbon dioxide reforming of methane over glow discharge plasma-reduced Ir/Al2O3 catalyst. Catalysis Communications, 2008, 9, 1558-1562.	3.3	58
89	Synthesis and Characterization of Noble Metal (Pd, Pt, Au, Ag) Nanostructured Materials Confined in the Channels of Mesoporous SBA-15. Journal of Physical Chemistry C, 2008, 112, 19818-19824.	3.1	156
90	Stability test and EXAFS characterization of plasma prepared Pd/HZSM-5 catalyst for methane combustion. Applied Surface Science, 2007, 254, 1506-1510.	6.1	14